

# Study on Crystallization of PVC/Graphene/Seashell Hybrid Biocomposites by Thermal and Hardness Analysis

Ferda Mindivan<sup>1,\*</sup>, Meryem Göktaş<sup>2</sup>, Hatice Bayrakçeken<sup>3</sup>

\*ferda.mindivan@bilecik.edu.tr

<sup>1</sup> Bilecik Şeyh Edebali University, Engineering Faculty, Department of Bioengineering, Bilecik, Turkey

<sup>2</sup> Bilecik Şeyh Edebali University, Vocational College, Department of Metallurgy, Bilecik, Turkey

<sup>3</sup> Department of Chemical Engineering, Faculty of Engineering, Atatürk University, Erzurum, Turkey

Received: July 2024

Revised: November 2024

Accepted: December 2024

DOI: 10.22068/ijmse.3676

**Abstract:** Natural-reinforced hybrid composites, called eco-materials, "are increasingly important for protecting the environment and eliminating waste problems. In this study, hybrid biocomposites were produced by the colloidal mixing method using seashell (SS) as natural waste, two graphene derivatives (graphene oxide (GO) and reduced graphene oxide (RGO)) as filler material, and polyvinyl chloride (PVC) as the polymer matrix. The crystallization and mechanical properties of hybrid biocomposites were examined based on their thermal properties using TGA and DSC analysis. Compared to PVC/GO and PVC/RGO composites with identical weight percentages of GO and RGO, the PVC/GO composite exhibited superior thermal stability and crystallinity, resulting in elevated hardness values for the same composite. These results were attributed to the better interaction of GO with PVC due to the higher number of oxygen-containing functional groups in GO than in RGO. However, the PVC/RGO/SS hybrid biocomposites exhibited superior properties than PVC/GO/SS hybrid biocomposites. The greatest crystallinity values were 39.40% for PVC/RGO/SS-20 compared to PVC/RGO composite and 29.21% for PVC/GO/SS-20 compared to PVC/GO. The PVC/RGO/SS-20 hybrid biocomposite showed the greatest gain in hardness value, up 18.47% compared to the PVC/RGO composite. No significant change was observed in the melting and weight loss temperatures as the SS content increased; however, the crystallinity and glass transition temperatures in hybrid biocomposites increased as the SS content increased. All analysis results demonstrated the achievement of SS-graphene-PVC interactions, suggesting that SS waste could enhance the thermal and mechanical properties of biocomposite production.

**Keywords:** PVC Hybrid biocomposite, Graphene, Seashell, Crystallinity, Thermal Analysis.

## 1. INTRODUCTION

Innovative hybrid composites with plastics and natural wastes have attracted attention for global sustainability goals. Particularly, the strength and durability of graphene-plastic hybrid composites make them one of today's most dynamic industries [1]. Hybrid composite studies on PVC, which was chosen as the polymer in this study, focused on the mechanical, thermal, and electrical properties of the produced materials. The seashell (SS) is in calcium carbonate form, and PVC-based plastics with calcium carbonate were used in the production of window and furniture profiles for cost reduction. And also, it increases the elastic modulus and hardness and improves the quality of the product's surface [2, 3]. Latest studies on PVC hybrid composites for example; Adediran et al. (2021) tested a hybrid PVC composite with treated bamboo fiber and particle coconut shell. They tested its tensile, flexural, elasticity, hardness, thermal and electrical conductivity, impact, and compressive strengths.

Researchers reported a consistent reduction in thermal conductivity with increased fiber loading, but only a slight increase with increased particulate loading [4]. Junqian Yang et al. (2024) synthesized and examined the characteristics of PVC composites filled with hybrid attapulgite filled with walnut shell powder. This indicates that attapulgite filling is a simpler, more efficient, and ecologically friendly way to improve the qualities of composites than alkali treatment [5]. Oluwagbenga et al. (2024) used plantain fiber (PF) and calcite particles (CP) in different weight percentages to create environmentally friendly PVC composites for use in automotive applications. The researchers made compression molding at 150°C for 10 minutes and analyzed the mechanical and thermal properties of the resulting composites. The results showed that the inclusion of these reinforcements significantly enhanced the composites' properties compared to unreinforced samples, with the hybrid composites exhibiting the best performance. These findings suggest that the developed hybrid biocomposite compositions

hold enormous promise for various applications [6]. Yang et al. (2024) reported on the properties of WS/PVC hybrid composites with walnut shell powder (WS) and attapulgite (ATP). They produced the composites using single-screw melt extrusion to compare the effects of various reinforcements. It also analyzed the composites' chemical composition, microstructure, thermal stability, mechanical, physical, and wear resistance properties [7]. Dutta and Maji (2023) developed a biobased composite using waste rice husk ash (RHA) and polyvinyl chloride in a 1:1 ratio. Using epoxidized soybean oil (ESO) as a green compatibilizer and tannic acid-calcium oxide (TA-CaO) nanocomposite as a thermal stabilizer made it possible to make the composites without using any solvents and in an eco-friendly way. The inclusion of graphene oxide (GO) nanomaterial enhanced the composite's mechanical, chemical, thermal, and flame-resistant qualities [8]. Shanmugasundar et al. (2020) investigated the PVC/glass fiber/graphene nanocomposite manufacturing process using traditional molding techniques. The matrix exhibited uniform graphene dispersion, which improves bonding. This study investigated the mechanical properties of the produced nanocomposite. The composites were created as flat test samples for use in pipes [9]. Allahbakhsh et al. (2020) produced PVC/rice husk hybrid composites with modified graphene oxide nanosheets. The addition of graphene oxide nanosheets modified by sodium dodecylbenzenesulfonate (SDBS) increased the viscosity of the melt mixture of PVC and rice straw compounds. The microstructural properties of the compounds improved as a result of this modification in the melt mixing rheology improved the compounds' microstructural properties [10]. Skórczewska et al. investigated chicken shells as a biofiller for creating composites made of unplasticized poly (vinyl chloride) in 2022. They reported that the biofiller significantly improved thermal stability. Furthermore, in PVC composites, the elastic modulus and softening point (VST) values increased significantly. They discovered that ground hen egg shells serve as an effective filler for PVC composites [3].

The authors decided to examine the thermal properties of eggshells and seashells due to their similar contents in this study. And also, the term "biocomposite" in this study refers to the

utilization of SS. Because the availability of waste SS is growing daily in coastal regions across the globe, Proper use of these SS can significantly improve the environment by lowering raw material costs and improving biocompatibility [11]. In addition to the authors' previous studies on GO and RGO, which examined the structural properties of unplasticized PVC/GO/SS [12] and unplasticized PVC/RGO/SS hybrid biocomposites [13], Because of the different oxygen-containing functional groups of GO and RGO, the structural properties of hybrid composites will be different, as well as their thermal properties. In this paper, the thermal properties of unplasticized PVC/GO/SS, and unplasticized PVC/RGO/SS hybrid composites were characterized by TGA and DSC. The best amounts of graphene derivative and SS were chosen based on the thermal analysis results.

## 2. EXPERIMENTAL PROCEDURES

In our previous studies, PVC/GO/SS [12] and PVC/RGO/SS [13] hybrid biocomposites were produced. Table 1 presents the composition of GO, RGO, and Sea Shell (SS), as well as the sample codes of the PVC/GO/SS and PVC/RGO/SS hybrid biocomposites utilized in this research.

Thermogravimetric analysis (TGA, STA 409, Netzsch) and differential scanning calorimetry analysis (DSC, STA 409, Netzsch) were performed by heating the samples from 20 to 600°C at a rate of 10°C min<sup>-1</sup> in a nitrogen atmosphere.

The degree of crystallinity ( $X_c$ ) of polyvinyl chloride (PVC) and hybrid biocomposites was determined using differential scanning calorimetry (DSC) and computed using Equation (1) and Equation (2), respectively.


$$X_c(\%) = \frac{\Delta H_c}{\Delta H_f} * 100 \quad (1)$$

$$X_c(\%) = \frac{\Delta H_c}{\Delta H_f(1-W_f)} * 100 \quad (2)$$

$\Delta H_c$  is the heat fusion of the samples obtained from DSC analysis,  $\Delta H_f$  is the fusion enthalpy of 100% crystalline PVC ( $\Delta H_f = 10.5$  J/g) [14] and  $W_f$  is the mass fraction.

In the previous studies on PVC/GO the synthesis, thermal, and structural characterization of composites, the authors obtained fusion enthalpy results for unfilled PVC by DSC analysis [15]. However, the degree of crystallinity was not determined in that particular investigation.

**Table 1.** wt.% of SS, GO, RGO and codes of biocomposites

	GO Content (wt%)	RGO Content (wt%)	SS Content (wt%)
PVC/GO	0.1	-	-
PVC/GO/SS-5	0.1	-	5
PVC/GO/SS-10	0.1	-	10
PVC/GO/SS-15	0.1	-	15
PVC/GO/SS-20	0.1	-	20
PVC/RGO	-	0.1	-
PVC/RGO/SS-5	-	0.1	5
PVC/RGO/SS-10	-	0.1	10
PVC/RGO/SS-15	-	0.1	15
PVC/RGO/SS-20	-	0.1	20

This study involved the computation of the crystallinity degree of unfilled PVC using Equation 1. In addition, Equation 2 was employed to determine the effect of incorporating GO, RGO, and various SS contents into the PVC matrix on the degree of crystallinity. The hardness test results were measured with Shore D hardness (WESTOP Type D-AB-0052-K). The hardness results reported in this work were averaged from 10 independent determinations.

The surface images of hybrid biocomposites were examined using a Nikon Eclipse LV150 optical metal microscope (OM) and scanning electron microscopy (SEM, Supra 40VP, Zeiss). Energy dispersive X-ray spectroscopy (EDS) analysis was also performed on the same device.

### 3. RESULTS & DISCUSSION

#### 3.1. TGA Analysis

Fig. 1 and Fig. 2 show the TGA weight loss and derivative thermograms of the PVC/GO, and

PVC/RGO hybrid biocomposites, respectively. They exhibited a three-step degrading process, as seen in Fig. 1 and 2. Due to the very small (0.1 wt%) incorporation of GO and RGO into the PVC matrix, the first-step decomposition temperatures of the PVC/GO and PVC/RGO composites were identical (Table 2).

The first step decomposition temperatures decreased in PVC/GO/SS-15 and PVC/GO/SS-20 hybrid biocomposites as seen in Table 2. All SS contents determined a decrease in PVC/RGO/SS hybrid biocomposites. This result is due to the amount of oxygen-containing functional groups of GO and RGO. Since GO has more oxygen-containing functional groups than RGO, GO-containing hybrid biocomposites showed a decrease in the temperature value of the first decomposition step at 15 wt.% and 20 wt.% SS content. Since RGO has fewer oxygen-containing functional groups, the initial decomposition temperature decreased in all SS-containing hybrid biocomposites compared to PVC/RGO composite.

**Table 2.** The decomposition temperatures of PVC/GO, PVC/RGO composites and their hybrid biocomposites

Sample	Decomposition Temperatures		
	First	Second	Third
PVC/GO	166.94	286.94	466.94
PVC/RGO	166.94	276.94	456.94
PVC/GO/SS-5	166.94	286.94	466.94
PVC/RGO/SS-5	156.94	286.94	466.94
PVC/GO/SS-10	166.94	286.94	466.94
PVC/RGO/SS-10	156.94	286.94	466.94
PVC/GO/SS-15	156.94	286.94	476.94
PVC/RGO/SS-15	156.94	286.94	466.94
PVC/GO/SS-20	156.94	286.94	466.94
PVC/RGO/SS-20	156.94	286.94	466.94

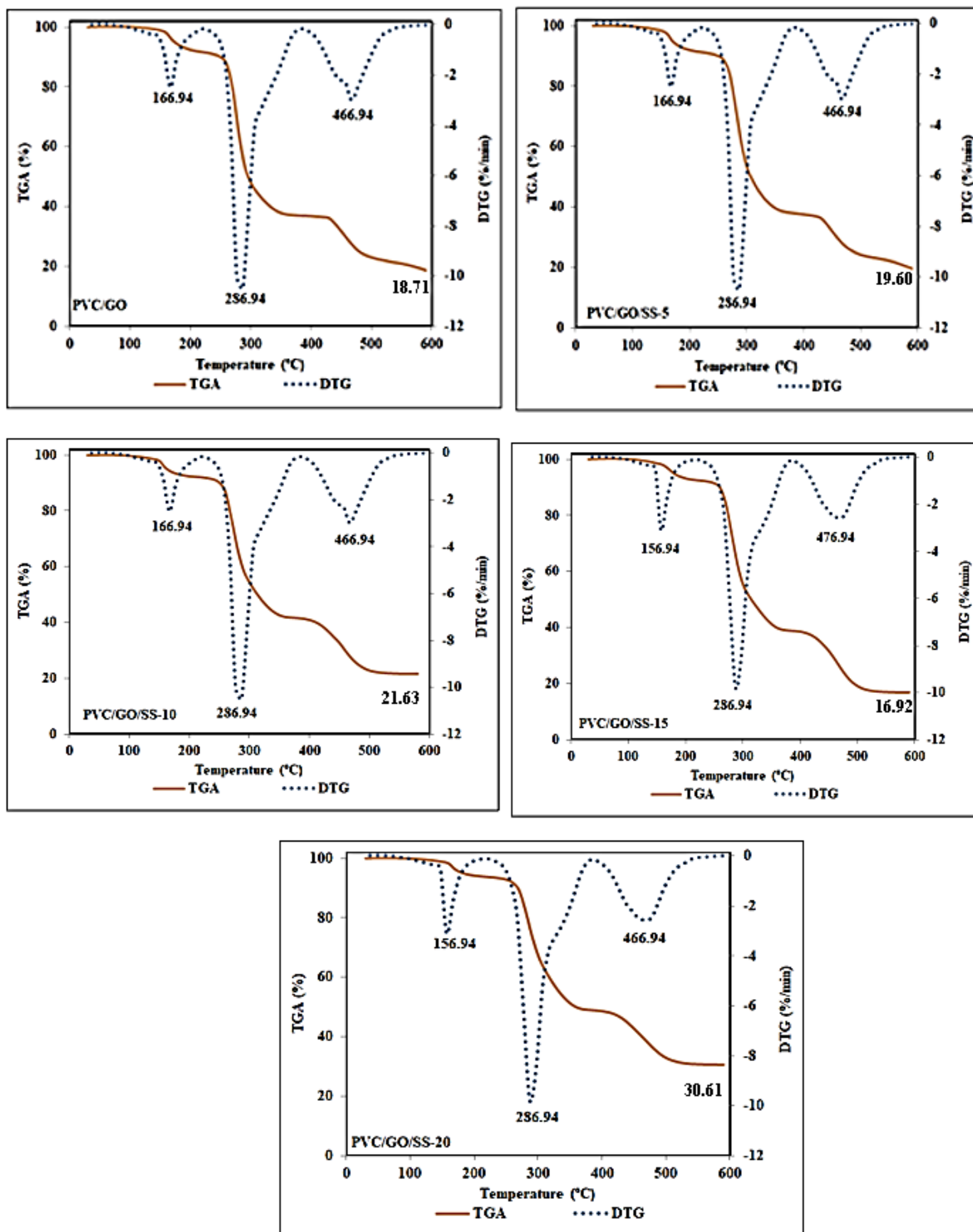
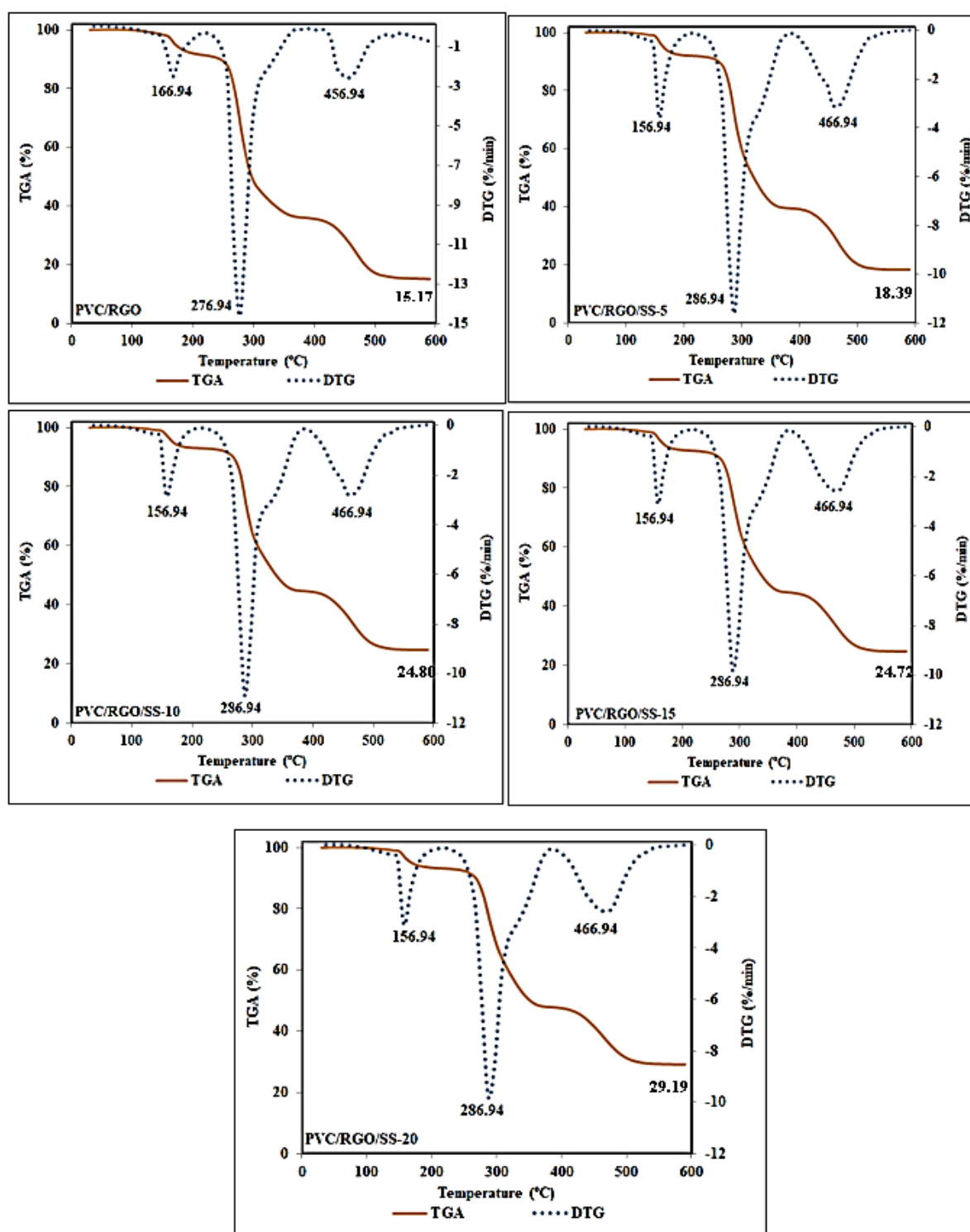


Fig. 1. TGA analysis results for the PVC/GO and PVC/GO/SS hybrid biocomposites

This decrease was due to the water-repellent property of the added SS. This result was the reason why the samples containing SS underwent first-step decomposition at lower temperatures. In the literature, the first region is characterized by the evaporation of physically weak, chemically

strongly bonded H<sub>2</sub>O molecules, as well as the evaporation of CO and CO<sub>2</sub> gases from polymers [16]. RGO also weakened the bonds in the PVC matrix due to the increased evaporation of H<sub>2</sub>O, CO, and CO<sub>2</sub> gases from polymers compared to GO.



**Fig. 2.** TGA analysis results for the PVC/RGO and PVC/RGO/SS hybrid biocomposites

The presence of more oxygen groups in GO facilitated the prevention of bond weakening. However, it was understood that this weakening occurred at the amounts of 15 and 20 wt.%. The de-hydrochlorination of PVC/GO/SS hybrid biocomposites attributed to that began at 286.94°C

in the second stage [17, 18, 19]. Fig. 1 suggests that adding all SS amounts to PVC did not significantly affect the onset de-hydrochlorination temperature. The second stage of degradation of PVC/RGO composites started at 276.94°C but increased up to 286.94°C for PVC/RGO/SS



hybrid biocomposites (Table 2). Although the thermal stability of the PVC/RGO composite (276.94°C) is lower than that of the PVC/GO composite (286.94°C), the thermal stability increased in all PVC/RGO/SS hybrid biocomposites with the addition of SS. The thermal stability is due to the addition of SS rather than RGO. The temperatures of all biocomposites increased from 276.94°C for PVC/RGO to 286.94°C. In the end, the C-Cl bonds in PVC/RGO weakened at this temperature, but SS reinforcement strengthened the weakened bond once more. The cleavage backbone of the polymer was responsible for the final degradation step [20], observed at 466.94°C for PVC/GO and 456.94°C for PVC/RGO composites (Table 2). Although the PVC/RGO composite's decomposition temperature is low, the degradation temperature values of PVC/RGO/SS hybrid biocomposites shifted to higher levels with the addition of SS, just like second step degradation, as seen in Fig. 2. Fig. 1 shows the decomposition temperature of the only PVC/GO/SS-15 hybrid biocomposite increased. The high residue amount at 600°C, which is another indicator of thermal stability, is effective in preventing the formation of volatile aromatic compounds. Previous studies conducted with PVC reported that composite samples with the highest residue amount also had high thermal stability [21, 22]. Fig. 1 and Fig. 2 revealed that hybrid biocomposites produced with the addition of 20 wt% SS increased thermal stability with the highest residual amounts. With residue amounts of 30.61% and 29.19%, respectively, PVC/GO/SS-20 and PVC/RGO/SS-20 hybrid

biocomposites demonstrated the highest thermal stability compared to other hybrid biocomposites and composite samples.

### 3.2. DSC Analysis

Fig. 3 and Fig. 4 show the DSC thermograms of the PVC/GO, PVC/RGO, and their hybrid biocomposites, respectively. The PVC/GO and PVC/RGO had a melting point of 250.26°C. There was a correlated degradation peak, with its center located at 250.26°C. Fig. 3 and Fig. 4 indicated that the melting point maximum values of all composites at 260.26°C were visible in the DSC curves of all of the PVC/GO/SS and PVC/RGO/SS hybrid biocomposites.

The melting temperature peaks of all hybrid biocomposites, as displayed in Figs. 3 and 4, broadened and shifted to higher temperatures with the SS addition. The interaction between SS and PVC/GO-PVC/RGO was attributed to the broad melting transition peak [23]. It was evident that the SS loading caused the melting point of PVC/GO and PVC/RGO composites to move to a higher temperature, independent of the different wt.% of SS. This might be explained by the common impact of the filler addition [24, 25], since SS prevented polymer chain movement by creating a hydrogen bond between the hydrogen groups of PVC chains and the hydroxyl groups on the edges of SS. The PVC/GO and PVC/RGO composites showed a glass-transition temperature ( $T_g$ ) of around 56.12 and 60.06°C, according to the DSC thermograms, respectively. However, as can be shown in Fig. 3 and Fig. 4, the  $T_g$  value of the PVC/GO/SS and PVC/RGO/SS hybrid biocomposites increased as the amount of SS increased.

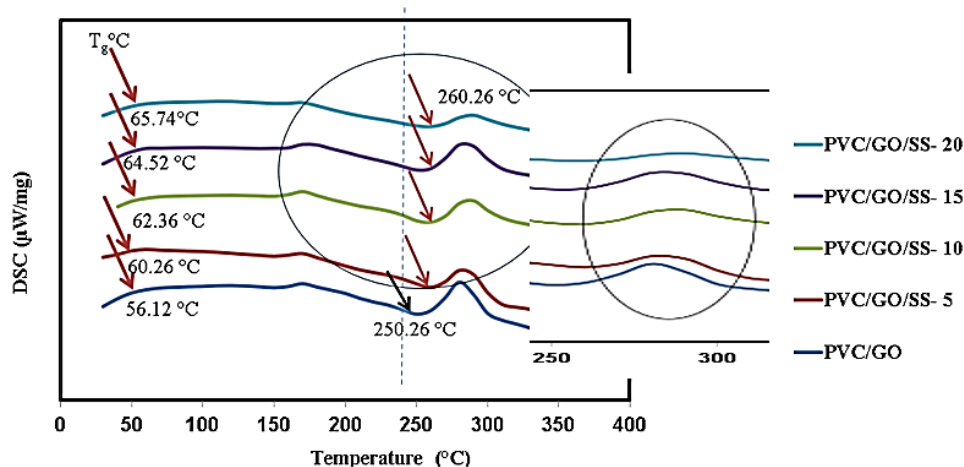


Fig. 3. DSC thermogram for the PVC/GO and PVC/GO/SS hybrid biocomposites

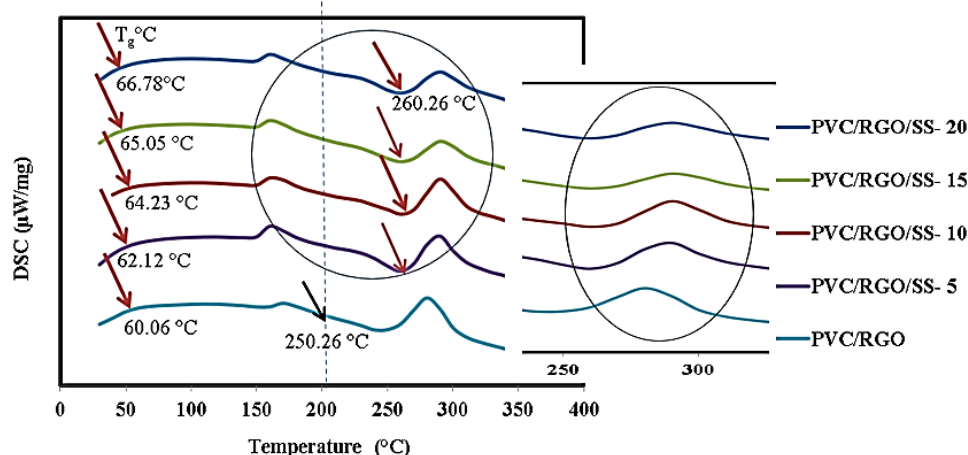


Fig. 4. DSC thermogram for the PVC/RGO and PVC/RGO/SS hybrid biocomposites

The increased  $T_g$  results from a distinct effect of SS distribution on temperature-dependent PVC chain mobility, where a better dispersion of SS led to a higher restriction of PVC chain motion [26]. In a previously reported reviewer study, the solvent casting method prepared PVC nanocomposites containing up to 20 wt.% of ZnO. According to the DSC analysis results, the  $T_g$  increased. The strong interaction was between ZnO nanoparticles and the PVC matrix [27]. Another study found that uniformly distributed  $\text{CaCO}_3$  nanoparticles, added to the PVC matrix at concentrations up to 5 wt%, had a similar temperature effect during in-situ polymerization. The simultaneous influence of the nanoparticles on the restriction of segmental and long-range chain mobility shifted the glass transition temperature of the PVC slightly towards higher values (about 1.1–1.4°C) compared to unfilled PVC [28]. Table 3 shows crystallite fusion enthalpy and the degree of crystallinity ( $X_c$ ) of the PVC/GO and PVC/RGO composites, and their hybrid

biocomposites. The author's previous study provided the enthalpy value for PVC [15]. This calculated value (5.58%) was consistent with the values found in the literature for commercial PVC [29]. Researchers had found enthalpy values of PVC/GO and PVC/RGO composites [12, 13]. In this study, the crystallinity values of all of them were found from Equation 1 and 2. Table 2 demonstrated an increase in crystallinity values ( $X_c$ ) as the wt% SS contents in hybrid biocomposites increase. It was understood that hybrid biocomposites with a 20 wt% SS addition had the highest crystal size values. Crystallinity values of 7.96% for PVC/RGO/SS-20 and 7.74% for PVC/GO/SS-20 were found. The highest crystallinity values were 29.21% for PVC/GO/SS-20 compared to PVC/GO and 39.40% for PVC/RGO/SS-20 compared to PVC/RGO. It has been reported in previous studies that these high crystallinity values will also increase the hardness of the samples [30, 31]. Therefore, Shore D hardness measurements of the samples were made.

Table 3. The crystallite fusion enthalpy and % $X_c$  of PVC/GO, PVC/RGO composites and their hybrid biocomposites

Sample	$\Delta H$ (J/g)	$X_c$ (%)
PVC/GO/SS-20	64,94	7,74
PVC/GO/SS-15	60,50	6,78
PVC/GO/SS-10	60,70	6,43
PVC/GO/SS-5	60,70	6,09
PVC/GO	62,9	5,99
PVC	58,66	5,58
PVC/RGO	59,95	5,71
PVC/RGO/SS-5	61,25	6,14
PVC/RGO/SS-10	61,39	6,50
PVC/RGO/SS-15	62,25	6,98
PVC/RGO/SS-20	66,86	7,96

### 3.3. Shore D Hardness Testing

The hardness values of the PVC/GO and PVC/RGO composites and their hybrid biocomposites are shown in Fig. 5. As seen in Fig. 5, the hardness value of unfilled PVC was determined to be 82.9. This value was found to be compatible with other PVC articles in the literature that use the same hardness scale [32, 33].

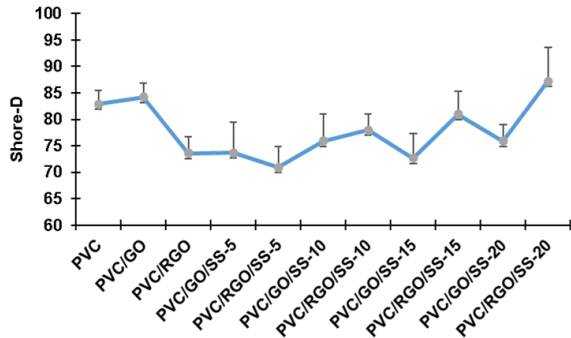


Fig. 5. Shore D hardness test results of the PVC/GO, PVC/RGO, and their hybrid biocomposites

Comparing the hardness values of PVC/GO and PVC/RGO composites revealed that the PVC/GO composite, with its higher degree of crystallinity (Table 3), also had a higher hardness value. Despite this, adding SS resulted in higher hardness values for PVC/RGO/SS hybrid biocomposites compared to those containing GO. And also, the crystallinity values are consistent with the results. The hybrid biocomposite coded PVC/RGO/SS-20 exhibited the highest improvement of 18.47% in hardness value compared to the PVC/RGO composite. Kumar et al. in their study where they added calcium carbonate to PVC resin, the shore D hardness of the composite with 22.36% calcium carbonate was found to be 87.0. In this study, the hardness value of PVC/RGO/SS-20 hybrid biocomposite was found to be 87.2 on the same hardness scale [33].

Fig. 6 shows the oxygen density distributed in the matrix as a result of the SEM-EDS elemental mapping analysis of hybrid biocomposites.

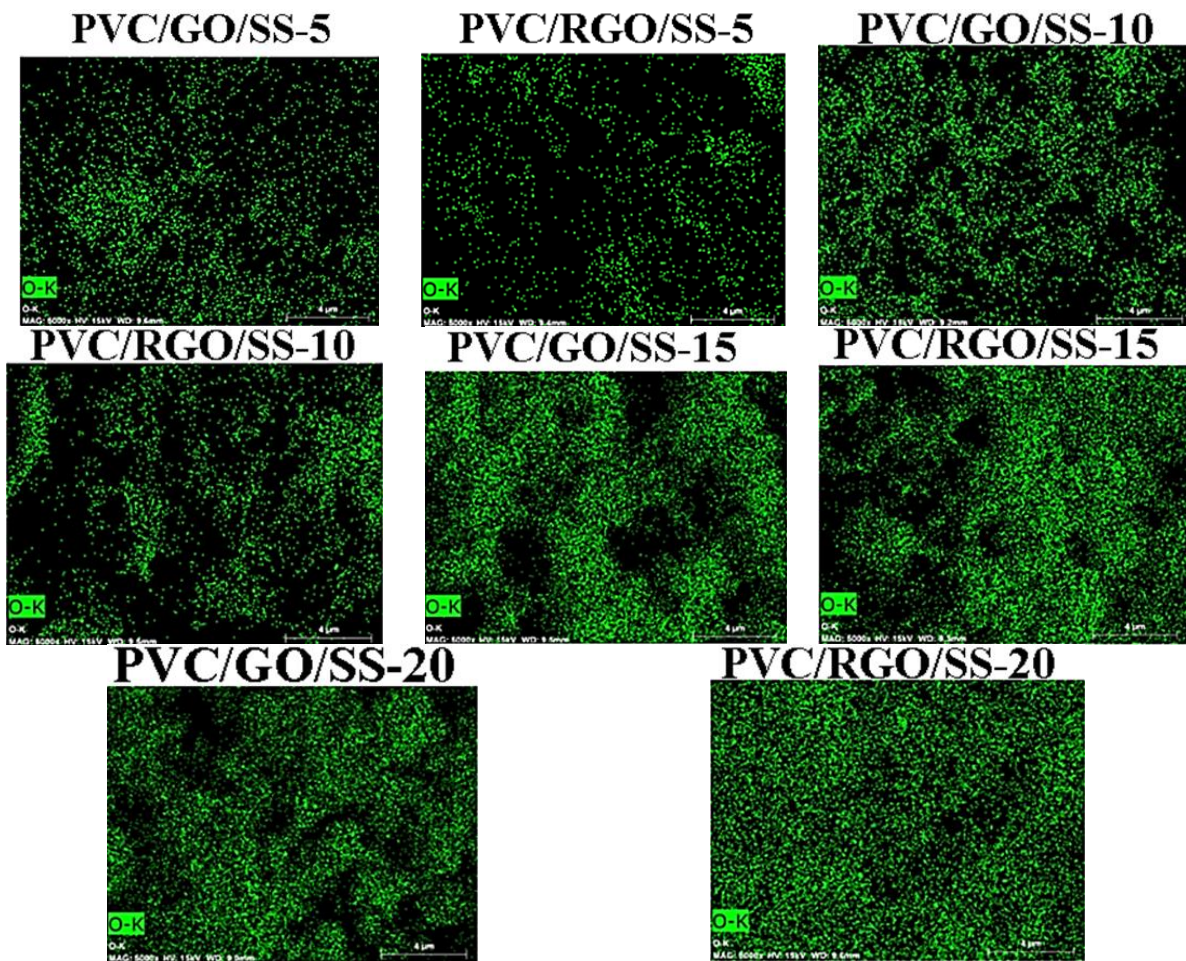


Fig. 6. SEM-EDS elemental mapping of hybrid biocomposites at same magnification (50X)



As the amount of SS increased, the oxygen concentration in the matrix increased. There are intermittent voids in all images. But it was observed least intermittent voids in the PVC/RGO/SS-20 hybrid biocomposite. This result is supported by the OM image of the same hybrid biocomposite in Fig. 7. In Fig. 7, as the SS amount increases in the OM images of the hybrid biocomposites, brighter and lighter colored traces of crystallinity are evident on the surface. These images also supported the increase in crystallinity (Table 3) and hardness (Fig. 5) of the PVC/RGO/SS-20 hybrid biocomposite. Pan et al.'s poly(L-lactide)-based biocomposite and Castilla-Cortazar's studies on the morphology, crystallinity, and molecular weight of poly(caprolactone)/graphene oxide hybrids yielded similar results [34, 35].

#### 4. CONCLUSIONS

In this study, the usability of waste Sea Shell (SS) as reinforcement material for hybrid biocomposites was examined. Its relationship with mechanical and structural properties, especially its effect on thermal properties due to its calcium carbonate content, has been

investigated. The TGA and DSC analysis results showed that adding SS during the three-step degradation increased the thermal stability with high residue amounts in hybrid biocomposites with the highest 20 wt% SS addition. The degree of crystallinity ( $X_c$ ) and the glass transition temperatures of hybrid biocomposites increased as the amount of SS increased. These results were attributable to the hydrogen bonds between the hydrogen groups of PVC chains and the hydroxyl groups on the edges of SS and GO-RGO, as well as the distribution of SS in the matrix. The addition of SS also had an effect on the hardness values. As the amount of SS increased, the hardness values also increased. The highest hardness value appeared in the PVC/RGO/SS-20 hybrid biocomposite at the highest wt.% SS value, just like the crystallinity degree. As a result, the addition of SS had an effect on thermal stability, crystallinity of the structure and hardness. Interaction and bonding between PVC-GO-RGO and SS was achieved. Therefore, the authors recommend using the fillers and reinforcements from this study to produce hybrid composites with high thermal stability and hardness.

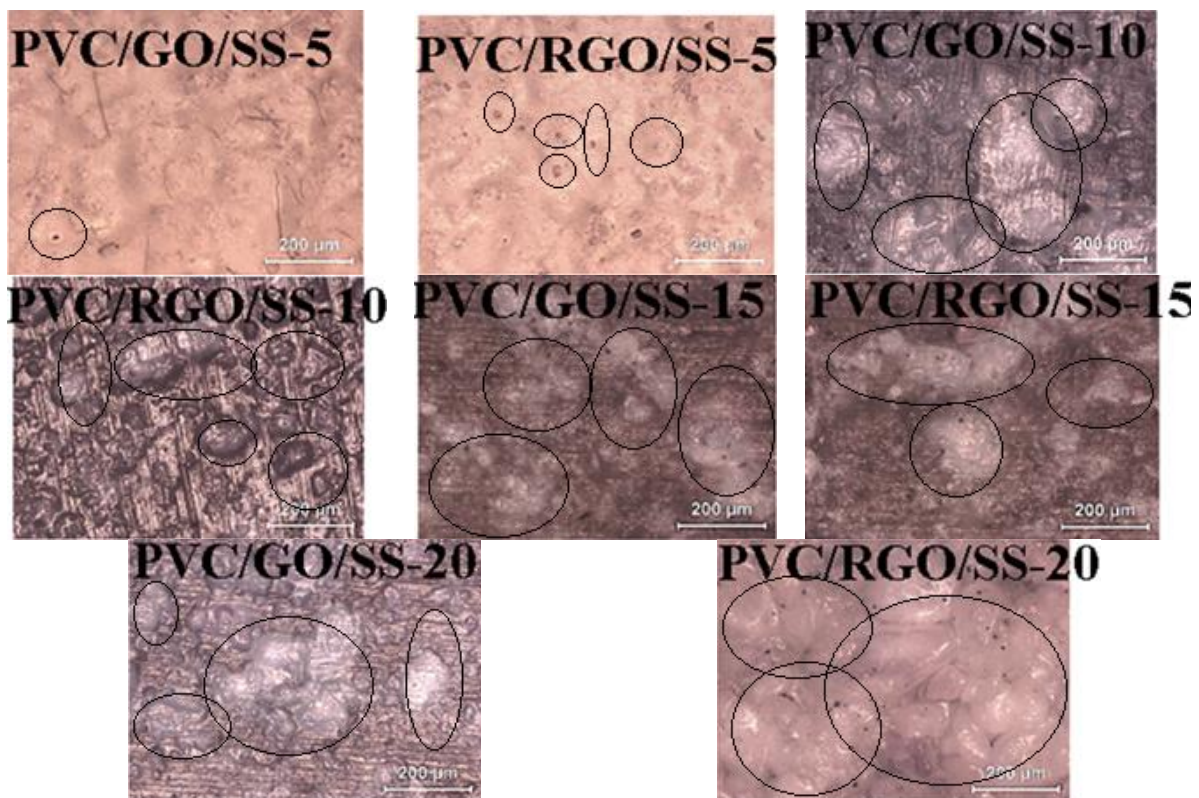


Fig. 7. OM images of hybrid biocomposites at same magnification (10X)

## CONFLICT OF INTEREST

There are no conflicts to declare including any competing financial interest.

## ACKNOWLEDGEMENTS

The authors are grateful to Bilecik Şeyh Edebali University, Bilecik, Turkey for authorization to carry out the research work. The authors gratefully acknowledge the financial support of the research foundation (Project no: 2019-01.BŞEÜ.03-02 and 2019-02.BŞEÜ.11-01) of Bilecik Şeyh Edebali University.

## REFERENCES

- [1]. Adhikary, K.B, Pang, S. and Staiger, M.P., “Dimensional stability and mechanical behaviour of wood–plastic composites based on recycled and virgin high-density polyethylene (HDPE).” *Compos. B. Eng.*, 2008, 39:807–815. <https://doi.org/10.1016/j.compositesb.2007.10.005>.
- [2]. Mindivan, F. and Göktaş, M., “Preparation of new PVC composite using green reduced graphene oxide and its effects in thermal and mechanical properties.” *Polym. Bull.*, 2020, 77, 1929–1949. <https://doi.org/10.1007/s00289-019-02831-x>.
- [3]. Skórczewska, K., Lewandowski, K., Szewczykowski, P., Wilczewski S, Szulc J, Stopa P and Nowakowska P., “Waste Eggshells as a Natural Filler for the Poly(Vinyl Chloride) Composites.” *Polymers*, 2022. 14, 20, 4372. <https://doi.org/10.3390/polym14204372>.
- [4]. Adediran, A.A., Akinwande, A.A., Balogun, O.A., Olasoju, O. S. and Adesina, O. S., “Experimental evaluation of bamboo fiber/particulate coconut shell hybrid PVC composite.” *Sci Rep.*, 2021. 11, 5465. <https://doi.org/10.1038/s41598-021-85038-3>.
- [5]. Yang, J., Zhang, K., Chen, D., Zhang, X. and Zhang, Y., “Preparation and properties of PVC composites filled with walnut shell powder hybrid attapulgate.” *Journal of Vinyl and Additive Technology*, 2024. 30, 1, 263-276. <https://doi.org/10.1002/vnl.22046>.
- [6]. Oluwagbenga, A.S., Oluwole, O.I., Ilesanmi, A., Akinlabi, O. and Olanrewaju, O.F., “Development of hybrid plantain fiber/calcite particles reinforced polyvinyl chloride biocomposites for automobile applications.” *Journal of Thermoplastic Composite Materials*. 2024, 37, 6, 1938-1956. <https://doi.org/10.1177/08927057231208143>.
- [7]. Yang, J., Zhang, K., Chen, D., Zhang, X. and Zhang, Y., “Preparation and properties of PVC composites filled with walnut shell powder hybrid attapulgate.” *J Vinyl Addit Technol*. 2024, 30, (1), 263-276. <https://doi.org/10.1002/vnl.22046>.
- [8]. Dutta, N and Maji, T.K., “Development of waste rice husk/PVC/GO nanocomposite using TA–CaO adduct and ESO as green additives.” *Journal of Thermoplastic Composite Materials*. 2023, 36, (5), 2212-2232. <https://doi.org/10.1177/08927057211063398>.
- [9]. Shanmugasundar, G., Vanitha, M., Babu, L. G., Suresh, P., Mathiyalagan, P., Krishnan, G. S., and Makos, M., “Fabrication and analysis of mechanical properties of PVC/Glass fiber/graphene nano composite pipes.” *Materials Research Express*. 2020, 7, (11), 115303. <https://doi.org/10.1088/2053-1591/abc277>.
- [10]. Allahbakhsh, A., “PVC/rice straw/SDBS-modified graphene oxide sustainable Nanocomposites: Melt mixing process and electrical insulation characteristics.” *Composites Part A: Applied Science and Manufacturing*. 2020, 134, 105902. <https://doi.org/10.1016/j.compositesa.2020.105902>.
- [11]. Jagatheeshwaran, M. S., Elayaperumal, A., and Arulvel, S., “Wear characteristics of electroless NiP/bio-composite coatings on En8 steel.” *Journal of Manufacturing Processes*, 2015, 20, 206-214. <https://doi.org/10.1016/j.jmapro.2015.08.002>.
- [12]. Göktaş, M. and Mindivan, F., “Grafen Oksit ve Deniz Kabuğu Takviyeli Polivinil Klorür Hibrit Kompozitlerin Karakterizasyonu.” *Avrupa Bilim ve Teknoloji Dergisi*, 2020. 20, 685-692. <https://doi.org/10.31590/ejosat.782828>.

- [13]. Mindivan, F., and Göktaş, M., "Production and characterization of graphene/PVC biocomposite from seashell wastes." *Materials Today: Proceedings.*, 2020, 27, 3119-3123.  
<https://doi.org/10.1016/j.matpr.2020.03.728>.
- [14]. Bao, Y., Weng, Z., Huang, Z., and Pan, Z., "The crystallinity of PVC and its effect on physical properties." *International Polymer Processing.* 1996, 11(4), 369-372.  
<https://doi.org/10.3139/217.960369>.
- [15]. Mindivan, F., "The Synthesis, Thermal and Structural Characterization of Polyvinylchloride/Graphene Oxide (PVC/GO) Composites", *Scientific Proceedings 1 International Scientific Conference "Material Science. Nonequilibrium Phase Transformations"*, Sofia, Bulgaria, 2015, 1310-3946.
- [16]. Alghunaim, N.S., "Spectroscopic analysis of PMMA/PVC blends containing CoCl<sub>2</sub>." *Results in Physics.*, 2015, 5, 331-336.  
<https://doi.org/10.1016/j.rinp.2015.11.003>.
- [17]. Jakić, M., Vrandečić, N. S. and Klarić, I., "Thermal degradation of poly (vinyl chloride)/poly (ethylene oxide) blends: Thermogravimetric analysis." *Polymer degradation and stability*, 2013, 98(9), 1738-1743.  
<https://doi.org/10.1016/j.polymdegradstab.2013.05.024>.
- [18]. Guangbao, W., Shangsuo, Y., and Jijun, X., "Thermal degradation kinetics of calcium stearate/PVC composite." *Results in Materials*, 2020, 8, 100-123.  
<https://doi.org/10.1016/j.rinma.2020.100123>.
- [19]. Altarawneh, S., Al-Harashsheh, M., Buttress, A., Dodds, C., and Kingman, S., "A thermo-kinetic investigation on the thermal degradation of polyvinyl chloride in the presence of magnetite and hematite." *Thermochimica Acta*, 2022, 718, 179390.  
<https://doi.org/10.1016/j.tca.2022.179390>.
- [20]. Alghunaim, N. S., "Spectroscopic analysis of PMMA/PVC blends containing CoCl<sub>2</sub>." *Results in Physics*, 2015, 5, 331-336.  
<https://doi.org/10.1016/j.rinp.2015.11.003>.
- [21]. Fang, Y., Wang, Q., Guo, C., Song, Y. and Cooper, P. A., "Effect of zinc borate and wood flour on thermal degradation and fire retardancy of polyvinyl chloride (PVC) composites." *Journal of Analytical and Applied Pyrolysis*, 2013, 100, 230-236.  
<https://doi.org/10.1016/j.jaap.2012.12.028>.
- [22]. Labuschagne, F.J., Molefe, D.M., Focke, W.W., Van der Westhuizen, I., Wright, H.C. and Royeppen, M. D., "Heat stabilising flexible PVC with layered double hydroxide derivatives." *Polymer Degradation and Stability*, 2015, 113, 46-54.  
<https://doi.org/10.1016/j.polymdegradstab.2015.01.016>.
- [23]. Yang, S., Lei, P., Shan, Y., and Zhang, D., "Preparation and characterization of antibacterial electrospun chitosan/poly (vinyl alcohol)/graphene oxide composite nanofibrous membrane." *Applied Surface Science*, 2018, 435, 832-840.  
<https://doi.org/10.1016/j.apsusc.2017.11.191>.
- [24]. O'Neill, A., Bakirtzis, D. and Dixon, D., "Polyamide 6/Graphene composites: The effect of in situ polymerisation on the structure and properties of graphene oxide and reduced graphene oxide." *European Polymer Journal*, 2014, 59, 353-362.  
<https://doi.org/10.1016/j.eurpolymj.2014.07.038>.
- [25]. Li, P., Chen, X., Zeng, J. B., Gan, L. and Wang, M., "Enhancement of the interfacial interaction between poly (vinyl chloride) and zinc oxide modified reduced graphene oxide." *RSC advances*, 2016, 6(7), 5784-5791.  
<https://doi.org/10.1039/C5RA20893A>.
- [26]. Sterzyński, T., Tomaszewska, J., Piszczek, K. and Skórczewska, K., "The influence of carbon nanotubes on the PVC glass transition temperature." *Composites Science and Technology*, 2010, 70(6), 966-969.  
<https://doi.org/10.1016/j.compscitech.2010.02.013>.
- [27]. Tomaszewska, J., Sterzyński, T., Woźniak-Braszak, A., Banaszak, M., "Review of Recent Developments of Glass Transition in PVC Nanocomposites." *Polymers.*, 2021, 13(24), 4336.  
<https://doi.org/10.3390/polym13244336>.
- [28]. Xie, X. L., Liu, Q. X., Li, R. K. Y., Zhou, X. P., Zhang, Q. X., Yu, Z. Z., and Mai,



- Y. W., "Rheological and mechanical properties of PVC/CaCO<sub>3</sub> nanocomposites prepared by in situ polymerization." *Polymer*, 2004, 45, (19), 6665-6673. <https://doi.org/10.1016/j.polymer.2004.07.045>.
- [29]. Aberoumand, M., Soltanmohammadi, K., Rahmatabadi, D., Soleyman, E., Ghasemi, I., Baniassadi, M., Abrinia K., Bodaghi M. and Baghani, M., "4D printing of polyvinyl chloride (PVC): a detailed analysis of microstructure, programming, and shape memory performance." *Macromolecular Materials and Engineering*, 2023, 308, (7), 2200677. <https://doi.org/10.1002/mame.202200677>.
- [30]. Xu, Y., Xiong, Y. and Guo, S., "Effect of liquid plasticizers on crystallization of PCL in soft PVC/PCL/plasticizer blends.", *Journal of Applied Polymer Science*, 2020, 137, (24), 48803. <https://doi.org/10.1002/app.48803>.
- [31]. López, J., Balart, R., and Jiménez, A., "Influence of crystallinity in the curing mechanism of PVC plastisols.", *Journal of applied polymer science*, 2004, 91, (1), 538-544. <https://doi.org/10.1002/app.13122>.
- [32]. Jeamtrakull, S., Kositchaiyong, A., Markpin, T., Rosarpitak, V., and Sombatsompop, N., "Effects of wood constituents and content, and glass fiber reinforcement on wear behavior of wood/PVC composites.", *Composites Part B: Engineering*, 2012, 43, (7), 2721-2729. <https://doi.org/10.1016/j.compositesb.2012.04.031>.
- [33]. Kumar, P.N., Nagappan, V., and Karthikeyan, C., "Effects of fly ash, calcium carbonate fillers on mechanical, moisture absorption properties in poly vinyl chloride resin.", *Materials Today: Proceedings*, 2019, 16, 1219-1225. <https://doi.org/10.1016/j.matpr.2019.05.217>.
- [34]. Pan, H., Kong, J., Chen, Y., Zhang, H., & Dong, L., Improved Heat resistance properties of poly (l-lactide)/basalt fiber biocomposites with high crystallinity under forming hybrid-crystalline morphology. *International journal of biological macromolecules*, 2019, 122, 848-856. <https://doi.org/10.1016/j.ijbiomac.2018.10.178>.
- [35]. Castilla-Cortázar, I., Vidaurre, A., Marí, B., and Campillo-Fernández, A. J., "Morphology, crystallinity, and molecular weight of poly (ε-caprolactone)/graphene oxide hybrids.", *Polymers*, 2019, 11(7), 1099. <https://doi.org/10.3390/polym11071099>.